THE ASTROPHYSICAL JOURNAL, 557:891–896, 2001 August 20
© 2001. The American Astronomical Society. All rights reserved. Printed in U.S.A.

WAITING-TIME DISTRIBUTIONS IN LATTICE MODELS OF SOLAR FLARES

JAMES P. NORMAN,[1] PAUL CHARBONNEAU, SCOTT W. MCINTOSH,[2] AND HAN-LI LIU
High Altitude Observatory, National Center for Atmospheric Research, P.O. Box 3000, Boulder, CO 80307
Received 2000 August 30; accepted 2001 April 26

ABSTRACT

It has recently been argued that the distribution of waiting times between successive solar flares is incompatible with the prediction of lattice models, which interpret flares as avalanches of magnetic reconnection events within a stressed magnetic structure driven to a state of self-organized criticality by stochastic motions of the photospheric magnetic footpoints. Inspired by a suggestion recently made by Wheatland, we construct modified lattice models driven by a nonstationary random process. The resulting models have frequency distributions of waiting times that include a power-law tail at long waiting times, in agreement with observations. One model, based on a random walk modulation of an otherwise stationary driver, yields an exponent for the power-law tail equal to 2.51 ± 0.16, in reasonable agreement with observational inferences. This power-law tail survives in the presence of noise and a detection threshold. These findings lend further support to the avalanche model for solar flares.

Subject headings: MHD — Sun: flares — Sun: magnetic fields

1. INTRODUCTION

It is generally agreed that solar flares are powered by magnetic energy stored in the form of electric currents flowing within complex magnetic structures embedded in the corona, in particular those overlying active regions. The observed short timescales for energy release, typically seconds to minutes, point to magnetic reconnection as the most likely mechanism of energy release (see Kulsrud 1998; Priest & Schrijver 2000; references therein). Although many aspects of the reconnection mechanism under solar coronal conditions remain poorly understood, it is clear that the time-varying electric fields generated in the course of a reconnection event have the ability to locally accelerate charged particles to superthermal velocities. It is the subsequent impact of these fast particles onto the colder surrounding plasma that leads, via bremsstrahlung, to the emission of hard radiation that is so spectacularly observed in X-ray solar images.

Solar X-ray and extreme-ultraviolet emission have been monitored almost continuously for nearly three decades now by various satellite-borne instruments. Those observations have revealed that the frequency distribution $f(E)$ of flare energy E follows a well-defined power law $f(E) \propto E^{-\alpha_E}$ over 8 decades in flare energy, with the value of the exponent α_E in the range 1.5–2.6, the actual value being sensitive to the adopted even selection criteria as well as to the physical and geometric assumptions made in converting observed fluxes to volumetric energy release (see, e.g., Crosby, Aschwanden, & Dennis 1993; Bromund, McTiernan, & Kane 1995; Krucker & Benz 1998; Aschwanden et al. 2000; references therein). A similar power law is obtained for the frequency distribution of peak flaring energy, i.e., $f(P) \propto P^{-\alpha_P}$, with $\alpha_P \simeq 1.8$. Interestingly, the values of these exponents are largely independent of the phase of the solar cycle (Dennis 1985; Crosby et al. 1993), which indicates that the flaring process is an intrinsic property of the coronal magnetic field rather than being controlled by an external driving mechanism such as magnetic flux emergence (although it is certainly well-established that flux emergence is a common *trigger* of the flaring process).

In their groundbreaking paper, Lu & Hamilton (1991; see also Lu et al. 1993; Lu 1995) demonstrated that the observed power-law distribution of flare energy release is well reproduced under the assumption that the solar corona is in a state of self-organized criticality (SOC; see Bak, Tang, & Wiesenfeld 1987; Jensen 1998; Sornette 2000). Physical systems in such a state undergo transitions between metastable states and, in so doing, release energy in the form of self-similar "avalanches." The system is said to be "critical" because its correlation length in response to perturbations spans the whole system. The critical state is said to be "self-organized" because no fine-tuning of the external parameter(s) is required, in contradistinction to classical thermodynamic phase transitions. Jensen (1998) argues that SOC can only materialize in slowly driven, interaction-dominated threshold systems. In fact, already reasoning along similar lines, Lu (1995) argued that the magnetic field overlying active regions meets these requirements.

In the papers mentioned above, Lu and collaborators have introduced what can perhaps now be called the "classical" SOC lattice model for solar flares (see also Vlahos et al. 1995; Galsgaard 1996; MacKinnon & Macpherson 1997; Georgoulis & Vlahos 1998; Charbonneau et al. 2001). Consider a three-dimensional regular cubic lattice, with each lattice node labeled by three integers, $\{i, j, k\}$. Now define on each lattice node a quantity B_{ijk} related to the magnetic field.[3] Enforcing $B = 0$ at all boundary nodes and starting from zero field throughout the lattice, small perturbations δB are added in succession to randomly selected interior nodes. After each such addition, the local

[1] Permanent address: Department of Physics, University of Newcastle upon Tyne, Newcastle upon Tyne NE1 7RU, UK.

[2] Present address: ESA Space Science Department, NASA Goddard Space Flight Center, Mail Code 682.3, Greenbelt, MD 20771.

[3] While identifying B_{ijk} with the magnetic field, Lu et al. (1993) also suggested an interpretation in terms of a magnetic vector potential. Isliker, Anastasiadis, & Vlahos (2000) have recently argued along similar lines and went on to show that energy dissipation in the model can then be interpreted as electrical current dissipation, a physically attractive scenario in the solar coronal context.

"tension" (ΔB) is computed:

$$\Delta B_{ijk} = B_{ijk} - \tfrac{1}{6} \sum_{nn} B_{nn} , \quad (1)$$

where the sum runs over the six nearest neighbors on the three-dimensional cubic lattice. Whenever this quantity exceeds some specified threshold B_c, something akin to reconnection is assumed to set in, and the field is locally redistributed according to the simple rule

$$B_{ijk} \to B_{ijk} - (\tfrac{6}{7}s)B_c, \quad B_{nn} \to B_{nn} + (\tfrac{1}{6}s)B_c , \quad (2)$$

with $s = \Delta B_{ijk}/|\Delta B_{ijk}|$. This redistribution may lead one or more of the nearest neighbor nodes to exceed the instability threshold, in which case the above redistribution rules are applied to the newly unstable nodes, and so on, as the "avalanche" propagates through the lattice, until stability has been restored everywhere.[4] Each redistribution event releases an amount of "magnetic energy"

$$E_{ijk} = \frac{6}{7}\left(2\,\frac{|\Delta B_{ijk}|}{B_c} - 1\right)B_c^2 . \quad (3)$$

A flare is then interpreted as the energy released collectively through the avalanche of redistribution events. The energy released by a single node just infinitesimally exceeding the stability threshold is

$$E_1 = \tfrac{6}{7}B_c^2 , \quad (4)$$

and is used below as a convenient energy unit.

Lu and collaborators went on to show that, provided a few simple criteria are met (namely, $\delta B/B_c \ll 1$; δB's extracted from a distribution with nonzero mean; and no perturbations added during an avalanche, implying a separation of timescales between the driving and the energy-release processes; see Lu et al. 1993 for further discussion), this simple system settles into an SOC state, with the frequency distribution of total and peak energy release in avalanches characterized by power-law distributions with indices $\alpha_E \simeq 1.5$ and $\alpha_P \simeq 1.8$, both in good agreement with observational inferences.

The waiting-time distribution (WTD) of solar flares is the distribution of time intervals Δt between successive flares. Observational determinations of the WTD have so far yielded varying results, depending on the range of wait times considered and event selection procedure adopted. For wait times longer than a few hours, the observed WTD is well described by a power law $f(\Delta t) \propto (\Delta t)^{-\alpha_{\Delta t}}$. Boffeta et al. (1999) find $\alpha_{\Delta t} = 2.4 \pm 0.1$ in soft X-rays, while Wheatland (2000) finds $\alpha_{\Delta t} = 2.16 \pm 0.05$ for the same data set but with a more restrictive selection criterion. The observational WTD is in direct conflict with the prediction of the lattice model described above, which yields an exponential WTD compatible with Poisson statistics (Wheatland, Sturrock, & McTiernan 1998). However, Wheatland (2000) has shown that the observed WTD can be understood in terms of a piecewise-constant Poisson process with an exponential distribution of flaring rates. He has presented a simple illustrative example to support this view, based on a Bayesian determination of the flaring rate from the data, and further suggested that a nonstationary lattice model could, in principle, reproduce the observed WTD.

In this paper, we present and discuss the statistical properties of two lattice models, relying on a simple modification of the driving mechanism used in the original formulation of Lu and collaborators. Both models yield a WTD with a power-law tail for large waiting times, and one of them reproduces reasonably well the observationally inferred value of the WTD power-law index in the long wait-time regime. This is a robust result, in that the power-law tail still materializes with approximately the same index in the presence of noise and detection threshold.

2. A LATTICE MODEL WITH NONSTATIONARY DRIVING

The perturbations added to the lattice are more than just the triggering mechanism for avalanches; they are the means through which energy is added to the lattice. The SOC state is stationary in the sense that, on average, avalanches dissipate as much energy as is added to the lattice in between avalanches, and the mean field set up across the lattice neither grows nor decays. Upon adding a perturbation δB to lattice site $\{ijk\}$, the lattice energy changes by an amount $\Delta E = (B_{ijk} + \delta B)^2 - B_{ijk}^2 \simeq 2B_{ijk}\,\delta B$, since typically $\delta B \ll B_{ijk}$ in the SOC on any reasonably sized lattice. Hence, the mean rate of energy input to the system is proportional to the mean of the δB distribution. However, an SOC system can dissipate energy either in numerous small avalanches, or in fewer larger ones. How the energy input rate relates to the avalanching rate is not a priori obvious in such models.

In the original model of Lu et al. (1993), the perturbations δB added to the lattice are extracted from a sequence of random deviates (r) uniformly distributed in the interval $[-0.2,0.8]$ (which implies a nonzero mean value $\langle r \rangle = 0.3$). The choice $B_c = 7$ then ensures that the system is being slowly driven, in the sense that $\delta B/B_c \ll 1$. To introduce nonstationarity in the driving rate, we retain these bounds and parameter values here but modulate the sequence of δB's by a time-dependent function $\rho(t)$ related to a one-dimensional random walk function:

$$\delta B = r\rho(t), \quad r \in [-0.2,0.8] . \quad (5)$$

We consider three distinct cases for $\rho(t)$, amounting to increasing nonstationarity:

1. Case I: $\rho(t) = 1$ is our reference case, namely, the scalar version of the Lu et al. (1993) model. In this case the flaring rate is expected to be well described by Poisson statistics (Wheatland et al. 1998; Wheatland 2000).
2. Case II: $\rho(t)$ is the square root of the absolute value of the random walk function.
3. Case III: $\rho(t)$ is the absolute value of the random walk function.

In the latter two cases, the random walk step size is chosen to be 10^{-2}, i.e., much smaller than the mean value of the random deviate distribution. One random walk step is taken each time a new δB is generated. Figure 1 shows the

[4] Equation (2) is the scalar equivalent of the redistribution rules used in Lu et al. (1993), who defined a *vector* field $\boldsymbol{B}_{ijk}$ at each lattice node. It has since been shown that, given the form of the driving used, the vector character of the field has no influence on the resulting statistical properties of the SOC model (see, e.g., Robinson 1994; Edney, Robinson, & Chisholm 1998). Most subsequent SOC work in the solar flares context has thus been carried out using a *scalar* quantity defined at each lattice node, which is computationally less demanding. Following Vlahos et al. (1995), we proceed here with the scalar version of the model.

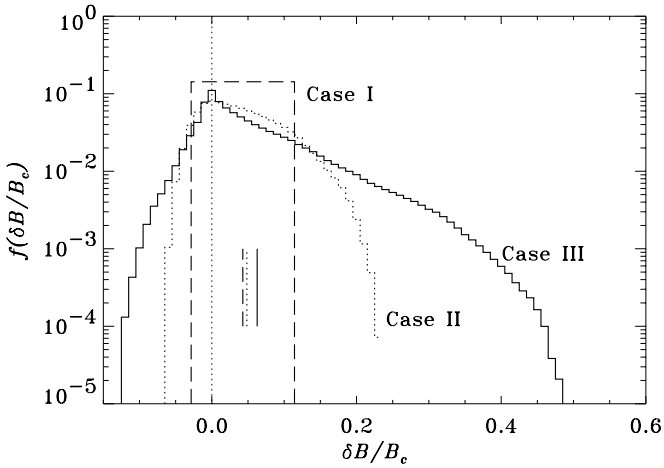

FIG. 1.—Normalized frequency distribution of field increments δB for representative realizations (of length 4×10^6 iterations) of the three drivers defined in § 2. The vertical line segments indicate the corresponding mean values for each case.

resulting distributions of field increments δB for representative runs of cases I, II, and III. For cases II and III, the width of the distributions is dependent to some degree on the random walk realization, but the distributions shown in Figure 1 are typical.

3. RESULTS

3.1. *Statistical Properties of the Nonstationary Lattice Models*

Starting with $B_{ijk} = 0$ throughout the lattice and enforcing this initial value as a boundary condition at the lattice edges, all three models are driven according to their respective $\rho(t)$ until a stationary state is attained. In all cases this state is characterized by avalanches of all sizes, with frequency distributions of total energy release (E), peak energy release (P), and duration (T) described by power laws, a canonical signature of SOC. All simulations are carried out on a 32^3 lattice. Numerical values for the corresponding power-law indices α_E, α_P, and α_T are listed in the first three rows of Table 1. Each entry is the average index obtained from fifteen independent runs, each of 4×10^6 iterations and involving about 2×10^5 avalanches. The error estimates are the rms deviation about the corresponding mean values. This ensures that the listed values are representative of the statistical properties of our various drivers $\rho(t)$. These values also depend somewhat on the adopted lattice size, but the results reported in Lu et al. (1993) indicate that the power-law indices remain reasonably stable for lattice sizes of 24^3 and higher (see their Table 1). For each individual run, the three indices are obtained by a nonlinear least-squares fit to a power law with an exponential rollover, as expected from finite size scaling arguments (see Lu et al. 1993, their § 2.2 and references therein):

$$f(X) = X^{-\alpha_X} \exp(-X/X_c) , \tag{6}$$

where X_c is a cutoff associated with the finite size of the lattice and X stands for either E, P, or T. As can be seen from Table 1, the frequency distributions are significantly steeper in the nonstationary cases.

3.2. *Waiting-Time Distributions*

Figure 2 summarizes results for the WTD for each of our three cases. The top panels show the distribution of perturbations δB added to the lattice over 2×10^6 iterations, together with a running mean (*thick solid line*). The bottom panels show the WTDs $f(\Delta t)$ constructed from the corresponding time series of energy release in the model. As found earlier by Wheatland et al. (1998), case I (Fig. 2*d*) is well fitted by an exponential distribution of waiting times, $f(\Delta t) \propto \exp(-\lambda_0 \Delta t)$, with the net mean flaring rate λ_0 directly determined from the entire energy release time series. Case II is characterized by a distribution of flaring rate that is approximately exponential except at low flaring rates (high Δt). This suggests a comparison with the model put forth by Wheatland (2000), who has shown that the theoretical WTD associated with a nonstationary but piecewise constant Poisson process with exponential distribution of rates takes the form

$$f(\Delta t) = 2\lambda_0/(1 + \lambda_0 \Delta t)^3 , \tag{7}$$

where once again λ_0 is the observed mean flaring rate. The dashed line in Figure 2*e* is equation (7) with λ_0 determined from the time series. At low Δt (high flaring rates), the agreement between Wheatland's formula and the case II WTD is indeed quite good.

The WTD for case III is shown in Figure 2*f*. Beyond waiting times of 20 (iteration units), the WTD is well fitted by a power law with index $\alpha_{\Delta t} = 2.51 \pm 0.16$, spanning over 2 orders of magnitude in Δt. Within the error bars, this value is in agreement with the observational inference of Boffeta et al. (1999), although significantly larger than the value 2.16 ± 0.05 reported by Wheatland (2000).

Figure 3 is a scatter plot of the mean flaring rate $\langle \lambda \rangle$ (i.e., number of flares per iteration, independent of flare size or duration) and mean energy release rate $\langle E_{\rm av} \rangle$ (mean energy released per iteration) versus mean rate of energy injection into the lattice $\langle E_{\rm in} \rangle$ for the Case III simulation (Figs. 2*c* and 2*f*). The three mean rates are computed over a 5×10^4 iteration averaging window, excluding epochs of avalanches. The large scatter notwithstanding, the mean energy release rate is directly proportional to the mean energy input rate, as it must be in a stationary system. This scatter

TABLE 1

POWER-LAW INDICES IN LATTICE MODELS

Case	$\langle N \rangle / E_1$	α_E	α_P	α_T	$\alpha_{\Delta t}$
I.....	0	1.45 ± 0.01	1.70 ± 0.03	1.70 ± 0.03	Exponential
II.....	0	1.49 ± 0.04	1.74 ± 0.09	1.75 ± 0.04	3.16 ± 0.13
III.....	0	1.53 ± 0.03	1.80 ± 0.10	1.75 ± 0.06	2.51 ± 0.16
	2	1.48 ± 0.03	1.70 ± 0.10	1.76 ± 0.06	2.79 ± 0.16
	5	1.48 ± 0.03	1.72 ± 0.10	1.80 ± 0.04	2.75 ± 0.13
	10	1.48 ± 0.03	1.73 ± 0.10	1.77 ± 0.03	2.71 ± 0.20
	20	1.48 ± 0.03	1.73 ± 0.10	1.78 ± 0.03	2.75 ± 0.18

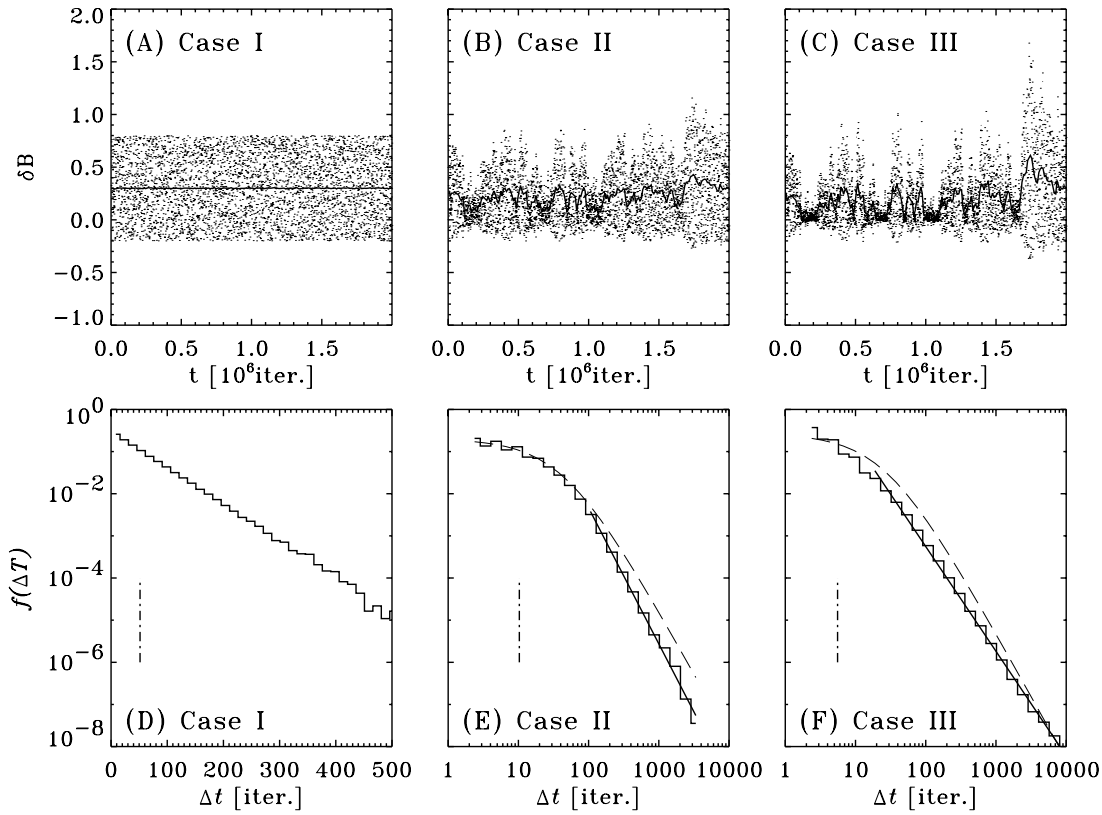

FIG. 2.—Summary of results for case I, II, and III simulations. The top panels show the distribution of perturbations δB added to the lattice, with the thick solid line corresponding to a running mean. The bottom panels show the WTDs constructed from the corresponding time series of energy release in the lattice after SOC has been reached. Note that the abcissa is linear for case I but logarithmic for cases II and III. The thick lines are power-law least-squares fits carried out for waiting time $\Delta t \geq 10^2$ (case II) and $\Delta t \geq 20$ (case III). The dash-dotted vertical line segment indicates the mean wait time over the full time series. The dashed lines correspond to eq. (6) of Wheatland (2000) with the mean flaring rate λ_0 computed directly from the time series. Wheatland's formula provides a good fit to the case II WTD for $\Delta t \lesssim 10^2$, but not to case III. The case III WTD power-law fit in the long waiting-time regime has an exponent -2.51 ± 0.16, in agreement within error bars with the observational inferences of Boffeta et al. (1999), but significantly larger than the value reported by Wheatland (2000).

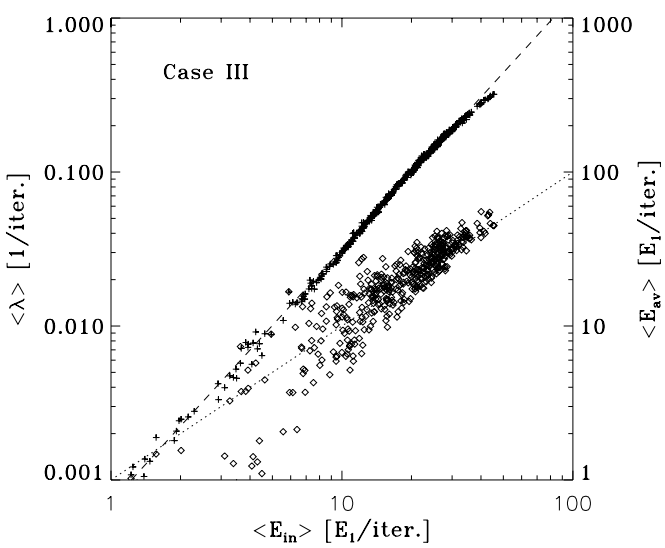

FIG. 3.—Mean flaring rate $\langle\lambda\rangle$ (*plus signs*; *left vertical axis*) and mean energy release rate $\langle E_{\rm av}\rangle$ (*diamonds*; *right vertical axis*) vs. mean energy input rate $\langle E_{\rm in}\rangle$ for a 4×10^6 iteration case III simulation. The means are computed over time series segments of 5×10^4 iterations, excluding avalanches and with 50% overlap between successive segments. The dashed line is a least-squares fit to a power-law relationship and yields an exponent equal to 1.64. The dotted line has a slope of unity, illustrating that $\langle E_{\rm av}\rangle$ is directly proportional to $\langle E_{\rm in}\rangle$, as it must be in a stationary state.

does reflect the fact that the system liberates energy in an intermittent, bursty manner, while the energy input rate is far more regular. On the other hand, the mean flaring rate increases with mean energy input rate as a remarkably tight power law with index 1.6 (Fig. 3, *dashed line*). This illustrates the fact that energy release in the SOC state occurs over a wide range of avalanche sizes, so that the mean flaring rate is not simply linearly proportional to the mean energy input rate. In fact, a larger value of $\langle E_{\rm in}\rangle$ does favor smaller flares at the expense of larger ones.

3.3. *Observational Threshold Effects*

The determination of the observed WTD for solar flares is greatly complicated by the existence of a detection threshold on the X-ray and/or extreme-ultraviolet flux, as well as by the finite spatial and temporal resolution of the observations themselves, which might cause two flares occurring closely in space and/or time to register as a single "event." In the framework of the lattice model, the situation in fact becomes even more complicated. A large flare is made up of a collection of small energy release events avalanching through a large portion of the lattice. One can define clusters of potentially unstable nodes as nodes where ΔB would exceed the instability threshold B_c if any neighboring node were to take part in an ongoing avalanche. Such clusters bear a strong morphological (and mathematical) resem-

blance to clusters within a percolating lattice near the percolation threshold (see Stauffer & Aharony 1994 for a nice introduction to the subject). In particular, such clusters are fractal objects with a highly inhomogeneous spatial structure. As a consequence, an avalanche sweeping through the cluster releases energy in a strongly fluctuating manner.

The histogram in Figure 4 (*thin black line*) shows a portion of the energy-release time series, including a moderately large avalanche. Assume now that the "count rate" of an instrument detecting this flare is linearly proportional to the energy release. Following Wheatland & Edney (1999), we now assume that a source of Poisson noise is present ($N(t)$, *thin gray line*) at an average level $\langle N \rangle$ (*dotted line*). The noise is added to the original time series, and a detection threshold Θ is set at a level corresponding to 3 σ above the mean, i.e., $\Theta = \langle N \rangle + 3\langle N \rangle^{1/2}$ (*dashed line*), a common procedure in analyzing real flare time series data (e.g., Bromund et al. 1995). The new "noisy" time series $E_N(t)$ is obtained by considering only counts above threshold Θ, i.e.,

$$E_N(t) = \begin{cases} E(t) + N(t) - \Theta\ , & \text{if } E(t) + N(t) > \Theta\ ; \\ 0\ , & \text{otherwise}\ . \end{cases} \quad (9)$$

Although the resulting time series bears a strong resemblance to the original noiseless time series, important differences materialize at low count rates. Two small flares (*b* and *c* in Fig. 4) no longer produce a signal above the threshold and so are lost. The final decay phase of the large flare is now fragmented, leading to two additional and apparently distinct events (points *d* and *e*). Finally, in instances where the noise does exceed the 3 σ level, an entirely spurious event can be produced in quiescent portions of the noiseless time series (such as event *a* in Fig. 4).

The consequences for the event-size and waiting-time frequency distributions are not immediately obvious. The noise addition and subsequent thresholding can add (*a*) or remove (*b*, *c*) small events, while the fragmentation of large avalanches can be expected to add smaller events (*d*, *e*), closely spaced in time, in a manner related to the fractal dimension of the time series. This evidently can affect all frequency distributions for the time series, including, in particular, the WTD.

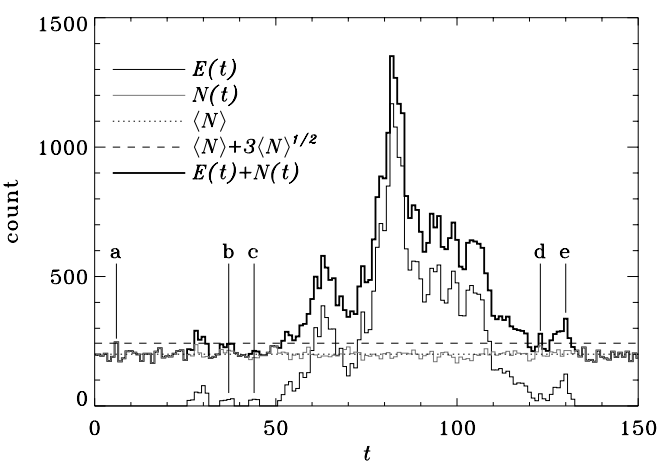

FIG. 4.—Effects of noise combined with a detection threshold on the energy release time series $E(t)$. The thin histogram is a portion of one such time series for a case III simulation, including a large avalanche. The thin gray histogram is synthetic Poisson noise $N(t)$, with mean $\langle N \rangle$ indicated by the dotted line. Adding this noise to the original time series leads to the thick histogram. A detection threshold is then set at $\Theta = \langle N \rangle + 3\langle N \rangle^{1/2}$. While the overall structure of the large avalanche is preserved, the number and temporal distribution of small amplitude events is strongly affected, which in turn affects the frequency distributions of event size, duration, and waiting times (see § 3.3 and Table 1).

The bottom four rows in Table 1 list the various power-law indices for a series of case III runs for various values of the assumed mean noise $\langle N \rangle$. The E, P, and T distributions are still power laws, but the index α_E is now nearly 2 σ smaller than the corresponding noiseless index (third row in Table 1). This suggests that in the presence of background noise, the power-law index α_E inferred from observations may be smaller than the corresponding indices characterizing the energy release within the flaring volume. The indices α_P and α_T are also smaller, and $\alpha_{\Delta t}$ larger, although the 1 σ ranges overlap comfortably with those of the noiseless case III time series.

With noise and threshold included, the WTD distributions also show small excesses of short wait times as compared with the original noiseless time series, especially for case II runs. While not compelling, this still offers some support to the explanation put forth by Wheatland et al. (1998) for the excess of short wait times seen in their sample of hard X-ray bursts, namely, that they are due to temporal structure within an energy release event, rather than to sympathetic flaring involving nonlocal physical mechanisms other than the purely local influences between neighboring flaring elements characterizing the lattice model.

4. DISCUSSION AND CONCLUSION

We have presented two nonstationary lattice models for solar flares that each yield a power-law behavior for the WTD at long wait times. Both models are characterized by frequency distributions of total energy release, peak energy release, and event duration that have the form of power laws, with power-law indices similar to those of the original stationary model of Lu and collaborators (our case I above).

In the first nonstationary model (case II), the distribution of driving perturbations is modulated by the square root of a random walk function. The theoretical WTD computed by Wheatland (2000) under the assumption of piecewise constant flaring *rates* provides a good fit to the model WTD except at low flaring rates. Our second nonstationary model (case III) is characterized by a WTD with a well-defined power-law tail at large waiting times, with the power-law index $\alpha_{\Delta t} = 2.51 \pm 0.16$ in reasonable agreement with observational inferences. The existence of a well-defined power-law tail is robust with respect to the introduction of noise and observational threshold on the energy-release time series from which the WTD is constructed, with only small variations of the power-law index.

While these results are encouraging from the point of view of lattice models for solar flares, one evidently needs to justify the introduction of nonstationary energy input to the system. Formally, no such justification exists at this writing, but again, neither does any exist for the strictly stationary driving used in the original lattice model of Lu et al (1993). In fact, given the observed tendency for magnetic flux emergence to recur on a relatively short timescale within existing active regions (e.g., Harvey & Zwaan 1983), it may well be that nonstationary driving is a better approximation to reality.

At any rate, the results presented herein show that it is relatively easy to produce lattice models that exhibit SOC

and are characterized by a WTD with a well-defined power-law tail at long wait times. We can but concur with Wheatland (2000) that it would be very premature at this juncture to abandon the SOC model in favor of explanatory constructs relying on intermittent energy dissipation in MHD turbulence (as put forth, e.g., by Boffeta et al. 1999). Energy dissipation in MHD turbulence does take place in an intermittent, bursty manner, involving the buildup of dissipative structures on a wide range of spatial scales (see, e.g., Longcope & Sudan 1994; Einaudi et al. 1996; Galsgaard & Nordlund 1996; Dmitruk & Gómez 1997; Galtier & Pouquet 1998). How this relates to magnetic energy dissipation in flaring active regions is a different matter. Except at times of flaring and/or flux emergence, the magnetic field above active regions appears to be in a more or less quiescent state, and—at least on observational spatial and temporal scales—shows no signature of fully developed MHD turbulence. Within a current sheet, however, MHD turbulence might play an important role in the reconnection process itself. Whether or not such turbulent effects can be represented by a suitably constructed SOC lattice model remains an intriguing question (see Einaudi & Velli 1999 for a discussion of this possibility).

J. P. N. thanks the High Altitude Observatory for a summer research internship. S. W. M. is supported through the Advanced Study Program at the National Center for Atmospheric Research (NCAR). H.-L. L. is partly supported through NASA grant S-97239-E to NCAR. We wish to thank an anonymous referee for very pertinent criticism of an earlier draft of this paper. The National Center for Atmospheric Research is sponsored by the National Science Foundation.

REFERENCES

Aschwanden, M. J., Tarbell, T. D., Nightingale, R. W., Schrijver, C. J., Title, A., Kankelborg, C. C., Martens, P., & Warren, H. P. 2000, ApJ, 535, 1047
Bak, P., Tang, C., & Wiesenfeld, K. 1987, Phys. Rev. Lett., 59, 381
Boffeta, G., Carbone, V., Veltri, P., & Vulpiani, A. 1999, Phys. Rev. Lett., 83, 4662
Bromund, K. R., McTiernan, J. M., & Kane, S. R. 1995, ApJ, 455, 733
Charbonneau, P., McIntosh, S. W., Liu, H.-L., & Bogdan, T. J. 2001, Sol. Phys., submitted
Crosby, N. B., Aschwanden, M. J., & Dennis, B. R. 1993, Sol. Phys., 143, 275
Dennis, B. R. 1985, Sol. Phys., 100, 465
Dmitruk, P., & Gómez, D. O. 1997, ApJ, 484, L83
Edney, S. D., Robinson, P. A., & Chisholm, D. 1998, Phys. Rev. E, 58, 5395
Einaudi, G., & Velli, M. 1999, Phys. Plasmas, 6, 4146
Einaudi, G., Velli, M., Politano, H., & Pouquet, A. 1996, ApJ, 457, L113
Galsgaard, K. 1996, A&A, 315, 312
Galsgaard, K., & Nordlund, Å. 1996, J. Geophys. Res., 101, 13445
Galtier, S., & Pouquet, A. 1998, Sol. Phys., 179, 141
Georgoulis, M. K., & Vlahos, L. 1998, A&A, 336, 721
Harvey, K. L., & Zwaan, C. 1993, Sol. Phys., 148, 85
Isliker, H., Anastasiadis, A., & Vlahos, L. 2000, A&A, 363, 1134
Jensen, H. J. 1998, Self-Organized Criticality (Cambridge: Cambridge Univ. Press), chap. 6
Krucker, S., & Benz, A. O. 1998, ApJ, 501, L213
Kulsrud, R. M. 1998, Phys. Plasmas, 5, 1599
Longcope, D. W., & Sudan, R. N. 1994, ApJ, 437, 491
Lu, E. T. 1995, ApJ, 446, L109
Lu, E. T., & Hamilton, R. J. 1991, ApJ, 380, L89
Lu, E. T., Hamilton, R. J., McTiernan, J. M., & Bromund, K. R. 1993, ApJ, 412, 841
MacKinnon, A. L., & Macpherson, K. P. 1997, A&A, 326, 1228
Priest, E. R., & Schrijver, C. J. 2000, Sol. Phys., 190, 1
Robinson, P. A. 1994, Phys. Rev. E, 49, 1984
Sornette, D. 2000, Critical Phenomena in Natural Sciences (New York: Springer), chap. 15
Stauffer, D., & Aharony, A. 1994, Introduction to Percolation Theory (2d ed.; London: Taylor & Francis)
Vlahos, L., Georgoulis, M., Kluiving, R., & Paschos, P. 1995, A&A, 299, 897
Wheatland, M. S. 2000, ApJ, 536, L109
Wheatland, M. S., & Edney, D. 1999, in NRO Report 479, Proc. Nobeyama Symposium, Solar Physics with Radio Observations, ed. T. Bastian, N. Gopalswamy, & K. Shibasaki (Nobeyama: Nobeyama Radio Obs.), 357
Wheatland, M. S., Sturrock, P. A., & McTiernan, J. M. 1998, ApJ, 509, 448